Quesada: A Framework for Reliable and Trustworthy Data Acquisition in 6G-IoT

Zhengzhe Xiang, Fuli Ying, Dezhi Wang, Rong Tan, Yufei Zhang, and Schahram Dustdar, *Fellow, IEEE*

***Abstract*—The convergence of artificial intelligence (AI) and the Internet of Things (IoT) in future sixth-generation (6G) networks (6G-IoT) promises to unlock unprecedented capabilities. However, the continuous collection and analysis of large-scale, low-density data pose significant threats to the reliability and trustworthiness of these systems, leading to high energy consumption and potential decision-making based on the stale information. To address these critical challenges, this article proposes a novel architecture for building reliable and trustworthy 6G-IoT services. Our approach involves three key contributions: 1) we leverage the multiaccess edge computing (MEC) paradigm to locally process raw data, filtering redundancy and thereby ensuring that AI models operate on more meaningful information; 2) we design a decoupled, two-level (edge–cloud) decision-making mechanism that explicitly manages the tradeoff between data trustworthiness (quantified by information freshness) and system energy consumption, a cornerstone of long-term reliability; and 3) we implement these principles in a new, distributed end–edge–cloud framework named query-control-based safe and data-trustworthy acquisition (Quesada), which coordinates edge and cloud decisions to enhance the overall system performance. To validate our approach, we conduct a series of comparative experiments. The results demonstrate that the Quesada framework significantly improves both system reliability and data trustworthiness, making it a viable architecture for future 6G-IoT applications.**

***Index Terms*—Data acquisition, multiaccess edge computing (MEC), trustworthy systems.**

NOMENCLATURE

$\mathcal{H}$	Set of edge servers $\mathcal{H} = \{h_1, h_2, ..., h_n\}$.
$\mathcal{V}_i$	Set of end devices $\mathcal{V}_i = \{v_{i,1}, \ldots, v_{i,m_i}\}$ connected to edge server h_i.
c	Cloud center in the sixth-generation Internet of Things (6G-IoT) system.
m_i	Number of end devices connected to h_i.
$\mathscr{D}_{i,j}$	Raw data sensed by end device $v_{i,j}$.
$\rho_{t,i,j}$	Edge decision variable: whether h_i collects data from $v_{i,j}$.
$\mathcal{G}_{t,i,j}$	Time slot index of the last data update for $\mathscr{D}_{i,j}$ at the edge.
$\mathcal{A}_{t,i,j}(\varsigma)$	Age of information (AoI) of $\mathscr{D}_{i,j}$ at moment ς, a metric for data trustworthiness.
δ	Duration of a time slot.
$q_{t,i,j}$	Cloud decision variable: probability of synchronizing $\mathscr{D}_{i,j}$.
$\ell_{t,i,j}$	Time cost of transferring data $\mathscr{D}_{i,j}$ to the cloud, a factor of system reliability.
$\mathrm{B}_{t,i,j}$	Data backlog of $\mathscr{D}_{i,j}$ stored in h_i.
$r_{t,i}$	Data transmission rate of edge server h_i.
$\eta_{i,j}$	Data generation rate for device $v_{i,j}$.
$\kappa_{i,j}$	Retention rate of previous data $\mathscr{D}_{i,j}$ at h_i.
γ	Weight coefficient balancing trustworthiness and reliability.
$B_i^\star$	Cache space limit of edge server h_i, a constraint for system reliability.
$\mathscr{D}_{i,j}^\dagger$	Edge's "view" of the data.
$\mathscr{D}_{i,j}^\circ$	Cloud's "replica" of the data.
$w_{t,i,j}$	Probability that the source data $\mathscr{D}_{i,j}$ changes.
$\mu_{i,j}$	Importance factor of data $\mathscr{D}_{i,j}$.
$\mathrm{D}^\star$	Cloud's synchronization capacity limit, a constraint for system reliability.
$\mathcal{L}_t$	Total transmission delay across the entire edge layer at time slot t.
$\mathscr{F}_t$	Data trustworthiness metric on the cloud side.
K	Scaling factor of the quantification method.

Received 26 June 2025; revised 10 August 2025 and 15 September 2025; accepted 3 October 2025. Date of publication 14 October 2025; date of current version 23 February 2026. This work was supported in part by the National Science and Technology Major Project under Grant 2022ZD0119103, in part by the National Natural Science Foundation of China under Grant 62102350, and in part by the Supercomputing Center of Hangzhou City University. *(Corresponding authors: Rong Tan; Yufei Zhang.)*

Zhengzhe Xiang, Fuli Ying, and Yufei Zhang are with Hangzhou City University, Hangzhou 310015, China (e-mail: xiangzz@hzcu.edu.cn; yingfuli@hzcu.edu.cn; zhangyf@hzcu.edu.cn).

Dezhi Wang is with Zhejiang University, Hangzhou 310058, China (e-mail: wangdezhi@zju.edu.cn).

Rong Tan is with Shanghai Business School, Shanghai 200235, China (e-mail: tanr@sbs.edu.cn).

Schahram Dustdar is with the Distributed Systems Group, TU Wien, 1040 Vienna, Austria, and also with ICREA, 08010 Barcelona, Spain (e-mail: dustdar@dsg.tuwien.ac.at).

Digital Object Identifier 10.1109/JIOT.2025.3621446

I. INTRODUCTION

AS COMMUNICATION systems evolve beyond 5G, the emerging 6G networks [1], [2] are poised to underpin a massive IoT ecosystem, enabling complex applications such as autonomous systems and smart cities. However, the unprecedented influx of data generated by these systems poses a significant challenge to the reliability and trustworthiness of the underlying AI models. The criticality of this challenge is underscored by recent regulatory initiatives, including the EU AI Act [3]. This article addresses a foundational aspect of this

issue: ensuring that AI models operate on data characterized by both freshness and reliable acquisition. To this end, we propose a novel framework within the Artificial IoT (AIoT) paradigm [4] to facilitate real time, trustworthy, and intelligent decision-making.

The range of 6G-IoT applications is expansive. For instance, in industrial manufacturing, AIoT-enabled nanorobots require highly reliable data streams for mission-critical automation. In Internet of Vehicles scenarios [5], [6], the development of 6G technology enables offloading vehicle tasks to multiaccess edge computing (MEC) deployed at the network edge, improving energy efficiency while ensuring the system performance [7]. Similarly, within smart cities, a cornerstone of the 6G vision, diverse municipal facilities integrated with AIoT technology demand trustworthy data to enhance the efficiency of public services and improve urban security [8], [9].

Nonetheless, the continuous, round-the-clock operation of 6G-IoT systems, characterized by the collection of large scale yet often low-density information, imposes a substantial burden that threatens their reliability and trustworthiness. On one hand, the immense energy consumption of perpetual data acquisition can compromise the operational lifetime of battery-powered devices, rendering the system fundamentally unreliable. On the other hand, processing a constant stream of redundant data leads to network congestion and high latency, forcing AI models to rely on stale information and thus making their decisions untrustworthy. This issue is particularly critical in applications that are not latency-sensitive but demand extreme availability and durability—key facets of reliability. For instance, in environmental monitoring, a significant portion of sensor data collected over short periods is often highly correlated or identical. Transmitting this redundant information creates a significant network burden and resource wastage, ultimately degrading the overall system reliability. Therefore, a critical challenge lies in architecting a trustworthy-by-design 6G-IoT system that intelligently manages data acquisition to jointly guarantee system reliability and decision trustworthiness. Reliability primarily refers to the system's ability to maintain stable operation under resource constraints. A reliable system can operate long term, stably, and efficiently, without easily failing due to resource exhaustion or overload. Trustworthiness refers to assessing the timeliness and accuracy of the data provided by the system, ensuring that decisions based on this data are credible. To this end, we propose a novel framework for reliable and trustworthy AI services. Our approach is twofold. First, we introduce a mobile edge computing-based architecture to perform local data processing. This strategy not only reduces transmission overhead but also acts as a first-line filter for redundant information, ensuring that data forwarded to higher level AI models is of greater informational value. Second, we design a two-stage adaptive frequency control mechanism that operationalizes trustworthiness. We theoretically model this by using information freshness (e.g., AoI) as a direct metric for data trustworthiness. We then formulate an optimization problem to balance this metric against energy constraints, thereby enhancing the system reliability. This theoretical model is engineered into a distributed decision-making process within our query-control-based safe and data-trustworthy acquisition (Quesada) framework, a new edge–cloud collaborative architecture designed for reliable and trustworthy 6G-IoT. The key contributions are summarized as follows.

1) We investigate and quantify the tradeoff between data collection strategies and data trustworthiness, measured by information freshness, establishing a foundational model for analyzing reliability in 6G-IoT data pipelines. Compared with existing works that mainly focus on energy consumption or only optimize the AoI in centralized scenarios, our model closely integrates the trustworthiness and reliability indicators.
2) We design a new architecture, named Quesada, by decomposing the complex data management problem into distributed subproblems. This distributed architecture enhances scalability and reliability, allowing for intelligent decision-making at both the edge and the cloud. This addresses the high energy consumption and high latency issues caused by redundant data transmission in traditional solutions.
3) We provide an evaluation and testing of our framework, demonstrating its superior performance in maintaining data quality and system reliability compared with representative baselines under various 6G-IoT-like settings. The results prove that our framework can quantify the tradeoff between information freshness and energy consumption, addressing the gap in the existing research regarding the co-optimization of trustworthiness and reliability.

The remainder of this article is organized as follows. In Section II, we present a concise yet illustrative example to motivate the research challenges addressed in this study. Section III systematically reviews prior work and establishes the theoretical foundation relevant to these challenges. Following this, Section IV formally defines the problem domain, including key concepts, assumptions, and mathematical formulations. Section V details the proposed methodologies, accompanied by rigorous theoretical analysis. Subsequently, Section VI evaluates the proposed approaches through comprehensive experiments, with a focus on algorithmic performance and sensitivity to critical parameters. Finally, Section VII summarizes the contributions of this work and outlines promising directions for future research.

II. Motivation and Scenarios

As previously discussed, data acquisition strategies are fundamental to system reliability and trustworthiness within the 6G-IoT context, particularly as requirements for data quality and energy efficiency vary. To illustrate the inherent tradeoffs, this section presents a concise yet representative example.

Consider a 6G-enabled smart farm scenario, depicted in Fig. 1, which features four edge servers (h_1, h_2, h_3, h_4). Each server connects to numerous sensors monitoring temperature, humidity, and illumination across the farmland. Within a given time frame, each edge server autonomously decides on its data collection and processing strategy before potentially uploading

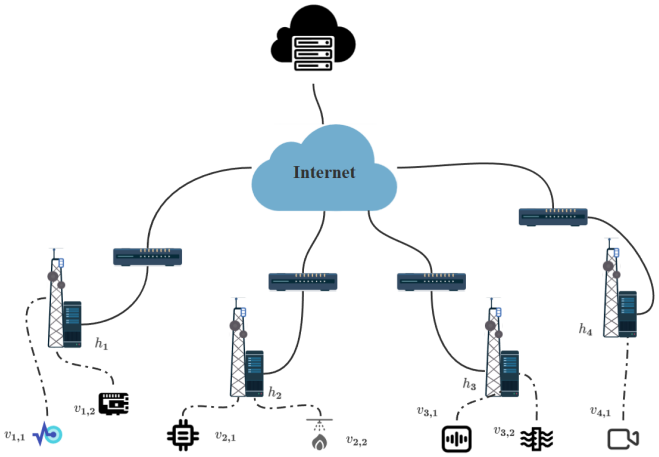

Fig. 1. Simple example of the system.

the cached data to the cloud for further analysis. This setup presents both the edge servers and the cloud with critical dilemmas concerning system trustworthiness and reliability:

Q1 (Scope of Data Collection): Is it necessary to query every end-device? In massive IoT deployments, an aggressive collection policy can rapidly deplete sensor batteries, compromising long-term operational availability and thus overall system reliability.

Q2 (Frequency of Data Synchronization): How often should data be synchronized with the cloud? An optimal frequency must be found to ensure data is fresh enough to be trustworthy for critical decisions (e.g., irrigation and pest control), without compromising the energy reliability.

The answers to these questions are inherently context-dependent, necessitating a tradeoff between competing objectives. It is therefore evident that an intelligent data acquisition approach is required to dynamically strike this balance. Such an approach forms the core of a trustworthy 6G-IoT architecture and will be the central focus of Section IV.

III. Related Works

Building reliable and trustworthy AI for 6G-IoT requires a multifaceted approach encompassing data acquisition, system architecture, and resource management. In this section, we review the literature across these key domains.

A. Information Freshness in Data Acquisition

The massive volume of data in 6G-IoT systems necessitates intelligent sensing and transmission strategies to ensure the communication reliability. A significant body of work focuses on the data volume reduction. For instance, Liazid et al. [10] and Singh and Nagaraju [11] proposed data aggregation and optimized routing to minimize transmissions, thereby enhancing the network stability. Similarly, others have applied algorithmic approaches like genetic algorithms to optimize clustering and routing for efficiency [12], [13]. While effective at reducing network load—a key component of reliability—these works primarily treat all data as homogeneous and do not explicitly model the trustworthiness of information, which is often time-sensitive. A more direct approach to data quality involves managing its freshness, commonly quantified by the AoI. The use of uncrewed aerial vehicles (UAVs) for data collection has become a popular scenario for AoI optimization. Works by Yi et al. [14] and Gao et al. [15] leverage reinforcement learning (RL) and ant colony algorithms, respectively, to optimize UAV trajectories for minimal AoI. Other studies focus on fairness, dynamic planning, and throughput maximization in UAV-assisted collection [16], [17], [18].

Based on a summary of the existing research, it is found that most studies focus on reducing data transmission to improve efficiency through methods such as data aggregation, routing optimization, and trajectory planning. Although these studies are crucial in establishing AoI as a critical performance metric, they often operate under the assumption of a centralized agent (UAV). Consequently, they neither address the distributed decision-making challenges inherent in a collaborative edge–cloud architecture nor do they fully integrate AoI as a driver for both edge-side data collection and cloud-side synchronization in a two-tiered system.

B. Edge–Cloud Architectures for Reliable 6G-IoT

MEC is widely recognized as a foundational architecture for 6G-IoT, bringing computation closer to data sources to enhance responsiveness and reliability. Research in this domain has heavily focused on computation offloading. Studies by Kai et al. [19], Tian et al. [20], and Huang et al. [21] proposed various collaborative frameworks and deep RL algorithms to optimize task placement (on device, edge, or cloud) to minimize latency and cost. Frameworks like SmartEye [22] demonstrate the practical benefits of edge–cloud collaboration for specific applications such as video analytics. While these architectural contributions are vital for building performant systems, their decision-making logic is typically driven by resource metrics like CPU load and network bandwidth, rather than the intrinsic trustworthiness of the data itself. The work by Long et al. [23] begins to explore an "end–edge–cloud" architecture for 6G but remains focused on traditional metrics like energy and delay.

Existing architectural studies primarily focus on computation offloading and resource allocation as core decision-making factors, optimizing latency and cost through collaborative frameworks or RL algorithms. However, the decision logic of these architectures does not center on data credibility (such as information freshness) as a driving factor, making it difficult to meet the demand for high-quality data from AI models in 6G-IoT. Therefore, there is an urgent need to develop an architectural paradigm where data acquisition and processing decisions are fundamentally guided by metrics representing data quality and trustworthiness.

C. System Reliability and Energy Management

The operational uptime of devices is a cornerstone of system reliability, especially in massive IoT deployments. Consequently, energy efficiency in MEC is a critical research area. For example, Li et al. [24] balanced computation

and communication energy in federated learning, while Li et al. [25] jointly optimized device trajectory and power. Other works employ RL [26] or optimization theory [27] to minimize the energy consumption for task execution. Furthermore, energy harvesting techniques have been explored to improve sustainability, a key aspect of long-term reliability. Chen et al. [7] proposed an efficient multivehicle task offloading algorithm based on 6G networks and the Cybertwin architecture, which realizes the optimization of dynamic task scheduling and resource allocation, minimizing the system cost while ensuring the stability of the task queue. Xia et al. [28], Zhou et al. [29], and Zhao et al. [30] proposed the sophisticated online algorithms to manage harvested energy alongside computation and offloading.

Although these studies significantly advance the state-of-the-art in making IoT systems more reliable from an energy perspective, they typically treat energy management as an independent optimization problem. The crucial link between the energy budget (a driver of reliability) and the required data freshness (a driver of trustworthiness) is largely overlooked. Optimizing for energy without considering its impact on information quality can lead to a reliable system that produces untrustworthy results.

In summary, the literature provides powerful tools for efficient transmission, MEC architectures, and energy management. However, these efforts often operate in silos. Few works holistically address the fundamental tradeoff between system reliability, driven by energy and resource constraints, and decision trustworthiness, driven by data freshness. Our work aims to bridge this critical gap. We propose a unified framework that not only incorporates these elements but also explicitly models and co-optimizes for both reliability and trustworthiness, using information freshness as a quantifiable metric within a novel, distributed edge–cloud architecture tailored for the challenges of 6G-IoT.

IV. Problem Description and Formulation

In this section, we establish a formal framework to model and optimize a reliable and trustworthy 6G-IoT system. Here, reliability refers to the system's ability to maintain stable operation under resource constraints; trustworthiness measures the timeliness and accuracy of the data provided by the system, ensuring that decisions made based on this data are credible. We begin by introducing the system model and the interactions between its entities. We then define a set of metrics to quantitatively measure data trustworthiness (via AoI) and system reliability (via resource utilization and latency). Finally, we formulate a unified optimization problem that captures the fundamental tradeoff between these two critical objectives. The notations are listed in the Nomenclature.

A. System Architecture

We consider a hierarchical architecture typical for 6G-IoT, which forms the basis of our proposed framework, Quesada. The system comprises a cloud center c, a set of edge servers $\mathcal{H} = \{h_1, \ldots, h_n\}$, and sets of end devices $\mathcal{V}_i = \{v_{i,1}, \ldots, v_{i,m_i}\}$ associated with each edge server h_i. We assume that devices connect to their nearest edge server, a common practice for minimizing latency [31], [32], [33]. The system operates in discrete time slots of duration δ, a standard approach for modeling control systems [34], [35]. Within this architecture, our goal is to design policies that govern the data flow from devices to the cloud, ensuring both reliability and trustworthiness. In Section IV, "data" are used throughout to describe the raw data sensed by the end devices.

B. Edge-Side Trustworthiness and Reliability Model

The edge server acts as a critical gatekeeper for data quality. Its primary role is to selectively collect data from end devices to maintain a fresh, trustworthy view of the world while operating within its resource limits to ensure system reliability. To quantify data trustworthiness, we employ the AoI, a widely adopted metric for information freshness in communication networks [36] and related systems [37], [38], [39]. Let $\rho_{t,i,j}$ be the binary decision variable for edge server h_i to collect data from device $v_{i,j}$ in time slot t

$$\rho_{t,i,j} = \begin{cases} 1, & h_i \text{ collects data from } v_{i,j} \text{ in the } t\text{-th slot} \\ 0, & h_i \text{ sleeps in the } t\text{th slot.} \end{cases} \tag{1}$$

The index of the last update slot, $\mathcal{G}_{t,i,j}$, is then given by

$$\mathcal{G}_{t,i,j} = \rho_{t,i,j} \cdot t + \left(1 - \rho_{t,i,j}\right) \mathcal{G}_{t-1,i,j}. \tag{2}$$

Consequently, the AoI of data $\mathscr{D}_{i,j}$ at any moment ς within the time slot is

$$\mathcal{A}_{t,i,j}(\varsigma) = \varsigma - \delta \cdot \mathcal{G}_{t,i,j}. \tag{3}$$

Assuming the cloud requests data $\mathscr{D}_{i,j}$ with probability $q_{t,i,j}$, the expected AoI for this data in slot t is $\mathcal{A}^*_{t,i,j}(\boldsymbol{\rho}_t)$. In the model, we assume that the probability of the cloud requesting edge data follows a uniform distribution within a single time slot. Therefore, $p(\tau)$ is the probability density function of the cloud requesting data $\mathscr{D}_{i,j}$ at time τ. This assumption is widely adopted in similar studies on information freshness, as it can reduce the complexity of model derivation [35], [40]. The derivation process of $\mathcal{A}^*_{t,i,j}(\boldsymbol{\rho}_t)$ is as follows:

$$\begin{aligned}
\mathcal{A}^*_{t,i,j}\left(\boldsymbol{\rho}_t\right) &= \underbrace{q_{t,i,j} \int_{\delta t}^{\delta t+\delta} \mathcal{A}_{t,i,j}(\tau)\, p(\tau)\, d\tau}_{\text{Trustworthiness when queried}} \\
&\quad + \underbrace{\left(1 - q_{t,i,j}\right) \mathcal{A}_{t,i,j}(\delta t + \delta)}_{\text{Trustworthiness when idle}} \\
&= q_{t,i,j} \int_{\delta t}^{\delta t+\delta} \mathcal{A}_{t,i,j}(\tau)\, \frac{1}{\delta} d\tau \\
&\quad + \left(1 - q_{t,i,j}\right) \mathcal{A}_{t,i,j}(\delta t + \delta) \\
&= q_{t,i,j} \frac{1}{\delta} \int_{\delta t}^{\delta t+\delta} \left(\tau - \delta \mathcal{G}_{t,i,j}\right) d\tau \\
&\quad + \left(1 - q_{t,i,j}\right) \left(\delta t + \delta - \delta \mathcal{G}_{t,i,j}\right) \\
&= \delta \left(q_{t,i,j} \left(t + \frac{1}{2} - \mathcal{G}_{t,i,j} \right) \right. \\
&\quad \left. + \left(1 - q_{t,i,j}\right) \left(t + 1 - \mathcal{G}_{t,i,j}\right) \right)
\end{aligned}$$

$$= \delta \left(1 - \frac{q_{t,i,j}}{2} + \left(1 - \rho_{t,i,j}\right)\left(t - \mathcal{G}_{t-1,i,j}\right)\right). \quad (4)$$

The total expected AoI, representing the overall data trustworthiness at the edge, is

$$\begin{aligned}\mathcal{A}_t^*\left(\boldsymbol{\rho}_t\right) &= \sum_{i=1}^{n}\sum_{j=1}^{m_i}\mathcal{A}_{t,i,j}^*\left(\boldsymbol{\rho}_t\right) \\ &= \sum_{i=1}^{n}\sum_{j=1}^{m_i}\delta\left(1 - \frac{q_{t,i,j}}{2} + t - \mathcal{G}_{t-1,i,j}\right) \\ &\quad - \delta\left(t - \mathcal{G}_{t-1,i,j}\right)\rho_{t,i,j} \\ &= \alpha_t + \sum_{i=1}^{n}\sum_{j=1}^{m_i}\beta_{t,i,j}\rho_{t,i,j} \end{aligned} \quad (5)$$

where α_t and $\beta_{t,i,j}$ are the constants for simplification. These constants primarily consist of parameters such as the time slot duration δ and the cloud decision variables $q_{t,i,j}$, which are independent of the optimization decisions. Consequently, they exert no influence on the subsequent optimization outcomes.

Next, we model system reliability, which is impacted by the transmission latency and resource constraints. The time cost, or latency, for uploading data $\mathscr{D}_{i,j}$ is

$$\ell_{t,i,j} = \rho_{t,i,j} \cdot \frac{\mathtt{B}_{t,i,j}}{r_{t,i}}. \quad (6)$$

In the calculation of the data backlog $\mathtt{B}_{t,i,j}$, a constant κ is introduced to represent the retention rate of historical data on the edge server. Over time, the freshness of historical data diminishes, leading to a reduction in its value. Consequently, the computation of the data backlog should not merely sum the historical backlog with newly generated data. Instead, the depreciation in the value of historical data must be accounted for. The data backlog $\mathtt{B}_{t,i,j}$ evolves according to

$$\mathtt{B}_{t,i,j} = \kappa \mathtt{B}_{t-1,i,j} + \rho_{t,i,j} \cdot \delta \cdot \eta_{i,j}. \quad (7)$$

The total transmission time cost, a key indicator of communication reliability, is

$$\mathcal{L}_t\left(\boldsymbol{\rho}_t\right) = \sum_{i=1}^{n}\sum_{j=1}^{m_i}\ell_{t,i,j}. \quad (8)$$

The edge-side objective is to balance the data trustworthiness and system reliability by minimizing their weighted sum

$$\Phi_t\left(\boldsymbol{\rho}_t\right) = \mathcal{A}_t^*\left(\boldsymbol{\rho}_t\right) + \gamma \mathcal{L}_t\left(\boldsymbol{\rho}_t\right). \quad (9)$$

This optimization is subjected to a critical reliability constraint: the cache capacity of each edge server must not be exceeded

$$\sum_{j=1}^{m_i}\mathtt{B}_{t,i,j} \le \mathtt{B}_i^{\star} \quad \forall h_i \in \mathcal{H}. \quad (10)$$

C. Cloud-Side Trustworthiness Maintenance

The cloud server maintains a replica $\mathscr{D}_{i,j}^{\circ}$ of the edge's cached view $\mathscr{D}_{i,j}^{\dagger}$. The core task for the cloud is to intelligently synchronize these replicas to ensure the trustworthiness of its global knowledge base, which serves as the foundation for high-level AI applications.

The effectiveness of the system hinges on the query strategy $\boldsymbol{q}_t = \{q_{t,i,j}\}$. An aggressive strategy (high $q_{t,i,j}$) ensures high data consistency but strains network resources, compromising reliability. A passive strategy (low $q_{t,i,j}$) saves resources but risks using stale, untrustworthy data. To model this, we define a cloud-side trustworthiness metric, $\mathscr{F}_t(\boldsymbol{q}_t)$, which measures the expected freshness of the cloud's data replicas

$$\begin{aligned}&\mathscr{F}_t\left(\boldsymbol{q}_t\right) \\ &= \sum_{i=1}^{n}\sum_{j=1}^{m_i}\mu_{i,j}\left(\underbrace{q_{t,i,j}}_{\text{Trustworthy if synced}} + \underbrace{\left(1 - q_{t,i,j}\right)\left(1 - w_{t,i,j}\right)}_{\text{Trustworthy if unchanged}}\right).\end{aligned} \quad (11)$$

Here, $\mu_{i,j}$ is an importance factor, and $w_{t,i,j}$ is the probability of the source data changing. The cloud aims to maximize this trustworthiness metric subject to its own reliability constraint—a finite data synchronization capacity $\mathtt{D}^{\star}$, which reflects the bandwidth or processing limits

$$\sum_{i=1}^{n}\sum_{j=1}^{m_i}\mathtt{B}_{t-1,i,j}q_{t,i,j} \le \mathtt{D}^{\star} \quad (12)$$

$$0 \le q_{t,i,j} \le 1. \quad (13)$$

D. Trustworthy-Reliable Data Acquisition Problem

Based on the analysis above, we can now formulate the unified optimization problem. We name it the trustworthy-reliable collaborative data acquisition (TR-CDA) problem. The goal is to find the optimal edge-side collection policy $\boldsymbol{\rho}_t$ and cloud-side synchronization policy $\boldsymbol{q}_t$ that jointly optimize a holistic utility function $\Psi(\boldsymbol{\rho}_t, \boldsymbol{q}_t)$, which integrates edge-side trustworthiness, system reliability, and cloud-side trustworthiness

$$\begin{aligned}\Psi\left(\boldsymbol{\rho}_t, \boldsymbol{q}_t\right) &= \mathcal{A}_t^*\left(\boldsymbol{\rho}_t\right) + \gamma\mathcal{L}_t\left(\boldsymbol{\rho}_t\right) - \delta\mathcal{F}_t\left(\boldsymbol{q}_t\right) \\ &= C_1\sum_{i=1}^{n}\sum_{j=1}^{m_i}\left(\delta\eta_{i,j}\rho_{t,i,j}^2 + \left(g_{t,i,j} + \gamma_{t,i,j}^{\kappa}\right)\rho_{t,i,j}\right. \\ &\qquad - \mu_{i,j}w_{t,i,j} + \mu_{i,j}w_{t,i,j}q_{t,i,j} \\ &\qquad \left. - \frac{1}{2}q_{t,i,j}\right) + C_2\end{aligned} \quad (14)$$

where C_1, C_2, $g_{t,i,j}$, and $\gamma_{t,i,j}^{\kappa}$ are terms for simplification. In this formula, C_2 is a coefficient unrelated to the decision variables, while C_1 is a simplified expression for coefficients related to the decision variables. Furthermore, this simplification process does not affect the optimization of the comprehensive utility function $\Psi(\boldsymbol{\rho}_t, \boldsymbol{q}_t)$. The TR-CDA problem, denoted by $\mathbf{P}_1$, is formally stated as follows:

$$\begin{aligned}\mathbf{P}_1 : &\min_{\boldsymbol{\rho}_t, \boldsymbol{q}_t} \ \Psi\left(\boldsymbol{\rho}_t, \boldsymbol{q}_t\right) \\ &\text{s.t. } (10), (12), (13).\end{aligned} \quad (15)$$

Solving $\mathbf{P}_1$ provides a principled way to navigate the complex tradeoffs in 6G-IoT, leading to a system that is both reliable in its operation and trustworthy in its AI-driven outcomes.

V. Problem Analysis and Solution

The formulated TR-CDA problem, $\mathbf{P}_1$, presents a complex, coupled optimization challenge. In this section, we first analyze its structure and explore a theoretically grounded solution using alternating minimization (AM). We then critically evaluate its practical limitations in a real-world 6G-IoT deployment, particularly its high computational complexity and centralized nature. This critique motivates our primary contribution in this section: a *decoupled, distributed, and efficient solution framework* that can be practically implemented on edge and cloud servers, thereby providing a viable pathway to building trustworthy-by-design systems.

A. Joint Optimization via AM

To make the joint optimization problem tractable, we introduce a key modeling assumption that links the edge-side collection policy to the cloud's view of data inconsistency. We posit that the probability of data modification, $w_{t,i,j}$, from the cloud's operational perspective, can be directly modeled by the edge's collection decision, $\rho_{t,i,j}$.

The rationale is crucial: the cloud's primary concern is not the physical change in the real world, but the information-state inconsistency between its replica $\mathscr{D}^{\circ}_{i,j}$ and the edge's latest view $\mathscr{D}^{\dagger}_{i,j}$. This inconsistency is precisely created at the moment the edge server decides to collect new data (i.e., $\rho_{t,i,j} = 1$). If the edge does not collect ($\rho_{t,i,j} = 0$), no new inconsistency is introduced from the cloud's perspective, as there is no new information at the edge to synchronize with. Therefore, this assumption models the probability of an actionable inconsistency that the cloud can potentially resolve

$$w_{t,i,j} = \rho_{t,i,j}. \tag{16}$$

This simplification is pivotal as it transforms the problem into a self-contained quadratic mixed-integer program (QMIP), enabling structured optimization. Consequently, optimizing $\Psi(\boldsymbol{\rho}_t, \boldsymbol{q}_t)$ is equivalent to optimizing

$$\psi\left(\boldsymbol{\rho}_t, \boldsymbol{q}_t\right) = \sum_{j=1}^{|\mathcal{V}_i|}\sum_{i=1}^{n}\left(\mathcal{X}_{i,j}\rho_{t,i,j}^2 + \mathcal{Y}_{t,i,j}\rho_{t,i,j} + \mathcal{Z}_{t,i,j}\rho_{t,i,j}q_{t,i,j} - \frac{1}{2}q_{t,i,j}\right) \tag{17}$$

where $\mathcal{X}_{i,j}$, $\mathcal{Y}_{t,i,j}$, and $\mathcal{Z}_{t,i,j}$ are the constants formed by combinations of coefficients related to the decision variables $\rho_{t,i,i}$ and $q_{t,i,j}$ within the time slot t.

Given its QMIP structure, we can adopt the AM approach. AM iteratively solves for one set of variables while keeping the other fixed.

1) *Fixing $\boldsymbol{\rho}_t$ to Solve for $\boldsymbol{q}_t$:* The problem reduces to $\mathbf{P}_\rho$, a standard linear programming (LP) problem, which can be solved efficiently using methods like method [41]

$$\mathbf{P}_\rho:\ \min_{\boldsymbol{q}_t}\ \sum_{j=1}^{|\mathcal{V}_i|}\sum_{i=1}^{n}\left(\mathcal{Z}_{t,i,j}\rho_{t,i,j} - \frac{1}{2}\right)q_{t,i,j}$$
$$\text{s.t. } (12), (13). \tag{18}$$

Algorithm 1 Solution With AM Method

Data: $\mathcal{H}, \mathcal{V}_i, \eta_{i,j}, r_{t,i}, \mathtt{D}^{\star}$
Result: $\boldsymbol{\rho}_t^*$, $\boldsymbol{q}_t^*$
Initialize $\boldsymbol{q}_t^* \leftarrow$ RAND(0,1)
// Set the max iterating round
for $i = 1$ *to* M **do**
  // Alternately optimizing
  $\boldsymbol{\rho}_t^* \leftarrow$ solve $\boldsymbol{P}_q$ with fixed $\boldsymbol{q}_t^*$
  $\boldsymbol{q}_t^* \leftarrow$ solve $\boldsymbol{P}_\rho$ with fixed $\boldsymbol{\rho}_t^*$
return $\boldsymbol{\rho}_t^*$, $\boldsymbol{q}_t^*$

2) *Fixing $\boldsymbol{q}_t$ to Solve for $\boldsymbol{\rho}_t$:* The problem becomes $\mathbf{P}_q$. Since $\rho_{t,i,j}$ is binary, we have $\rho_{t,i,j}^2 = \rho_{t,i,j}$, which linearizes the objective. The problem is thus transformed into an integer LP (ILP) problem

$$\mathbf{P}_q:\ \min_{\boldsymbol{\rho}_t}\ \sum_{j=1}^{|\mathcal{V}_i|}\sum_{i=1}^{n}\left(\mathcal{X}_{i,j} + \mathcal{Y}_{t,i,j} + \mathcal{Z}_{t,i,j}q_{t,i,j}\right)\rho_{t,i,j}$$
$$\text{s.t. } (10). \tag{19}$$

The overall AM procedure is outlined in Algorithm 1.

However, this centralized AM approach, while theoretically sound, faces two major barriers to practical deployment in 6G-IoT. First, the recurrent solving of ILP problems is computationally prohibitive for real-time decision-making. Second, it requires a central controller with global knowledge, which contradicts the distributed nature of edge computing and introduces significant communication overhead. These motivate the development of a more pragmatic, decoupled solution.

B. Decoupled Framework for Practical Implementation

To overcome the limitations of the centralized approach, we decompose the original problem into two independent, distributed subproblems that can be solved efficiently at the cloud and edge layers, respectively. This decomposition is the core of our Quesada.

1) Energy-Effective Cloud-Side Data Synchronization: The key to decoupling is to allow the cloud to estimate the data change probability $w_{t,i,j}$ without instantaneous knowledge of the edge's decision $\rho_{t,i,j}$. We achieve this by leveraging the principle of locality, using a historical average from a sliding window of size Δ

$$w_{t,i,j} = \frac{\sum_{\tau=t-\Delta}^{t}\mathbb{I}\left(\rho_{\tau,i,j} \neq 0\right)}{\Delta}. \tag{20}$$

With this approximation, the cloud's task becomes maximizing its data trustworthiness, as defined in $\mathscr{F}_t(\boldsymbol{q}_t)$, subject to its reliability constraint (synchronization capacity). This forms the cloud-side subproblem, $\mathbf{P}_C$

$$\mathbf{P}_C:\ \max_{\boldsymbol{q}_t}\ \sum_{j=1}^{|\mathcal{V}|}\sum_{i=1}^{n}\mu_{i,j}\left(\underbrace{q_{t,i,j}}_{\text{if sync}} + \underbrace{\left(1-q_{t,i,j}\right)\left(1-w_{t,i,j}\right)}_{\text{otherwise but not modified}}\right) \tag{21}$$

Algorithm 2 Cloud-Side Data Synchronization

Data: $B_{t-1,i,j}, w_{t,i,j}, \mu_{i,j}, \mathtt{D}^{\star}$
Result: $\boldsymbol{q}_t^*$
Initialize $\boldsymbol{q}_t \leftarrow \mathbf{0}$
Initialize $\mathtt{D} \leftarrow \mathtt{D}^{\star}$
Initialize $\mathcal{S} \leftarrow \left\{ \frac{\mu_{i,j} w_{t,i,j}}{\mathtt{B}_{t-1,i,j}} \right\}$
// Greedily search from the biggest value
while $\mathtt{D} > 0$ **do**
  $i^{'}, j^{'} \leftarrow \mathtt{IndexOfMaxElement}(\mathcal{S})$
  if $\mathtt{D} - B_{t-1,i^{'},j^{'}} \geq 0$ **then**
    $q_{t,i^{'},j^{'}} \leftarrow 1$
  // When unable to afford
  else
    $q_{t,i^{'},j^{'}} \leftarrow \frac{\mathtt{D}}{\mathtt{B}_{t-1,i^{'},j^{'}}}$
  $\mathtt{D} \leftarrow \mathtt{D} - q_{t,i^{'},j^{'}} \mathtt{B}_{t-1,i^{'},j^{'}}$
  $\mathcal{S}.\mathtt{remove}(\mu_{i^{'},j^{'}} w_{t,i^{'},j^{'}})$
return $\boldsymbol{q}_t^*$

$$\sum_{j=1}^{|\mathcal{V}|} \sum_{i=1}^{n} \mathtt{B}_{t-1,i,j} q_{t,i,j} \leq \mathtt{D}^{\star} \tag{22}$$

$$0 \leq q_{t,i,j} \leq 1. \tag{23}$$

The problem $\mathbf{P}_C$ is a classic example of the continuous knapsack problem (or fractional knapsack problem). The continuous knapsack problem refers to a scenario where there is a knapsack with a fixed capacity and several items, each having a specific weight and value. The goal is to select items to put into the knapsack such that the total value of the items in the knapsack is maximized, while not exceeding the knapsack's capacity constraint. Therefore, in the formulation of problem $\mathbf{P}_C$, each data source (i, j) can be regarded as an "item," corresponding to the item in the continuous knapsack problem. It has a "value" $\mu_{i,j} w_{t,i,j}$ and "weight" $\mathtt{B}_{t-1,i,j}$ and needs to be placed into a "knapsack" with a capacity of $\mathtt{D}^{\star}$. Here, the "data source" refers to the end devices. It is a well-established result in algorithm theory that this problem can be solved optimally by a greedy algorithm [42]. Algorithm 2 implements this optimal strategy by prioritizing items with the highest "trustworthiness density" $\mu_{i,j} w_{t,i,j} / \mathtt{B}_{t-1,i,j}$. Algorithm 2 synchronizes data sources by sorting and selecting those with the highest trustworthiness density. Therefore, the time cost of the algorithm is mainly concentrated on the sorting operation, and its time complexity is *O(nlog(n))*.

2) AoI-Driven Edge-Side Data Collection: With the cloud policy decoupled, each edge server h_i can independently decide its collection policy $\boldsymbol{\rho}_{t,i,*}$ to optimize its local objective: balancing data trustworthiness (AoI) and reliability (latency and cache usage). This forms the edge-side subproblem $\mathbf{P}_E$

$$\mathbf{P}_E : \min_{\boldsymbol{\rho}_t} \ \mathcal{A}_t^* \left(\boldsymbol{\rho}_t \right) + \gamma \mathcal{L}_t \left(\boldsymbol{\rho}_t \right) \tag{24}$$

$$\text{s.t. (10)}, \ \rho_{t,i,j} \in \{0, 1\}. \tag{25}$$

The objective function is linear in $\boldsymbol{\rho}_t$. Crucially, the problem is decomposable by the edge server. For each server h_i, we have an independent *0–1 knapsack problem*, $\mathbf{P}_E(i)$

$$\mathbf{P}_E(i) : \min_{\boldsymbol{\rho}_{t,i,*}} \ \sum_{j=1}^{|\mathcal{V}_i|} \left(\beta_{t,i,j} + \delta \gamma_{t,i,j}^{\kappa} + \frac{\gamma \delta \eta_{i,j}}{r_{t,i}} \right) \rho_{t,i,j} \tag{26}$$

$$\text{s.t.} \ \sum_{j=1}^{|\mathcal{V}|} \delta \eta_{i,j} \rho_{t,i,j} \leq \mathtt{B}_i^{\diamond}, \quad \rho_{t,i,j} \in \{0, 1\} \tag{27}$$

where $\mathtt{B}_i^{\diamond} = \mathtt{B}_i^{\star} - \kappa \sum_{j=1}^{|\mathcal{V}_i|} \mathtt{B}_{t-1,i,j}$, and $\rho_{t,i,j}$ indicates whether the j_th data source is selected. This problem is essentially a classic *0–1 knapsack problem*, which can be transformed into a maximization problem. Specifically, we can define the "value" of selecting item j as the negative of its "cost"

$$v_j = -\left(\beta_{t,i,j} + \delta \gamma_{t,i,j}^{\kappa} + \frac{\gamma \delta \eta_{i,j}}{r_{t,i}} \right). \tag{28}$$

The data size of item j as the "weight"

$$w_j = \delta \eta_{i,j}. \tag{29}$$

The objective becomes maximizing the total value under the constraint of satisfying the total weight limit. This problem can be solved in pseudo-polynomial time using dynamic programming (DP), but it is premised on the weights being integers. Therefore, before applying DP, we need to quantize the weights. The quantization process is implemented through an integer parameter K(scaling factor), converting the original problem into a new integer-based problem. Denote the new problem corresponding to edge server h_i as $\mathbf{P}_{\mathrm{QE}}(i)$

$$\mathbf{P}_{\mathrm{QE}}(i) : \max_{\boldsymbol{\rho}_{t,i,*}} \ \sum_{j=1}^{|\mathcal{V}_i|} v_j \rho_{t,i,j} \tag{30}$$

$$\text{s.t.} \ \sum_{j=1}^{|\mathcal{V}|} \left\lfloor K \delta \eta_{i,j} \right\rfloor \rho_{t,i,j} \leq \left\lfloor K B_i^{\diamond} \right\rfloor, \rho_{t,i,j} \in \{0, 1\}. \tag{31}$$

The new problem has integer weights and can be efficiently solved. For example, an original constraint of the form

$$0.12 \ x_1 + 0.5 \ x_2 + 0.4 \ x_3 \leq 2.$$

After multiplying by K with a value of 100, the original constraint is converted into an integer constraint

$$12 \ x_1 + 50 \ x_2 + 40 \ x_3 \leq 200.$$

After this transformation, the standard DP algorithm can be applied to find a high-quality approximate solution for the original problem. Algorithm 3 outlines this complete DP-based approach, which can be executed in parallel across all edge servers. In this process, there exists a tradeoff between solution accuracy and computational complexity. Next, we will conduct a theoretical analysis of the performance and complexity of this quantization method.

Assumption 1: Bounded Cost: Assume that the cost coefficient for each item j is bounded by a constant $C_{\max}$

$$\left| \beta_{t,i,j} + \delta \gamma_{t,i,j}^{\kappa} + \frac{\gamma \delta \eta_{i,j}}{r_{t,i}} \right| \leq C_{\max}. \tag{32}$$

This assumption is reasonable in 6G-IoT scenarios, as all parameters within the system (such as transmission rates and

Algorithm 3 Edge-Side Data Collection

Data: $\beta_{t,i,j}, \boldsymbol{\eta}_{i,j}, \gamma_{t,i,j}, \mathrm{B}_i^{\diamond}, r_{i,j}, \delta$
Result: $\boldsymbol{\rho}$

// Store the objective coefficients
$\mathcal{O} \leftarrow [\beta_{t,i,j} + \delta\gamma_{t,i,j}^{\kappa} + \frac{\gamma\delta\eta_{i,j}}{r_{t,i}}]_{j=1}^{|\mathcal{V}_i|}$
// Quantize the constraint coefficients
$\boldsymbol{\eta}_{i,*}, \mathrm{B}_i^{\diamond} \leftarrow \mathtt{quantize}(\boldsymbol{\eta}_{i,*}, \mathrm{B}_i^{\diamond})$
// Initialize DP table
$\mathtt{DP} \leftarrow [+\infty] * (\mathrm{B}_i^{\diamond} + 1)$
$\mathtt{DP}[0] \leftarrow 0$
for $j^{'}$ *from* 1 *to* $|\mathcal{V}_i| - 1$ **do**
  for b *from* $B_i^{\diamond}$ *to* $\eta_{i,j'}$ **do**
    $\mathtt{DP}[b] \leftarrow \min\left(\mathtt{DP}[b], \mathtt{DP}[b - \eta_{i,j'}] + \mathcal{O}_{j'}\right)$
$\mathtt{minVal} \leftarrow \min(\mathtt{DP}[\eta_{i,j'}:])$
// list the optimal solutions
Initialize $\boldsymbol{\rho} \leftarrow [0] * |\mathcal{V}_i|$
$b \leftarrow \mathtt{DP.indexOf(minVal)}$
for $j^{'}$ *from* $|\mathcal{V}_i|$ *to* 1 **do**
  if $b \geq \eta_{i,b} \cap DP[b] \equiv DP[b - \eta_{i,j'}] + \mathcal{O}_{j'}$ **then**
    $\rho[j^{'}] \leftarrow 1$
    $b \leftarrow b - \eta_{i,j'}$
return $\boldsymbol{\rho}$

Algorithm 4 Quantize-Solve-Repair (QSR)

Data: v, w, W, K
Result: $\boldsymbol{\rho_H}$

// Quantize weights and capacities
$w^{'} \leftarrow \lfloor K \cdot w \rfloor, W^{'} \leftarrow \lfloor K \cdot W \rfloor$
// Solving quantization problems using DP
$\rho_{approx} \leftarrow \mathtt{DP\_Solver}(v, w^{'}, W^{'})$
// Repair the solution
$\boldsymbol{\rho_H} \leftarrow \rho_{approx}$
while $\sum w_j \cdot \rho_{H,j} > W$ **do**
  $Minval \leftarrow minval(\rho_H)$
  $j^* \leftarrow \boldsymbol{\rho_H}.indexof(Minval)$
  $\boldsymbol{\rho_H}.remove(j^*)$
return $\boldsymbol{\rho}_H$

data generation rates) are finite physical quantities. Based on this, we can prove that the proposed quantization method (see Algorithm 4) has a bounded additive error.

Let V_{opt} be the optimal solution value of the original problem $P_E(i)$, V_{approx} be the optimal solution value of the quantization problem $P_{\text{EQ}}(i)$, and V_H be the feasible solution value obtained by Algorithm 4. Let S_{opt} be the optimal solution of $P_E(i)$, and S_{approx} be the optimal solution of the quantization problem. It can be derived that

$$V_{\text{opt}} \leq V_{\text{approx}}.$$

However, S_{approx} may violate the original capacity constraint. To satisfy the constraint, the repair step included in Algorithm 4 will gradually remove items with the lowest value density until the constraint is met. The final feasible solution obtained is $S_H \subseteq S_{\text{approx}}$, and its value is expressed as follows:

$$V_H = V_{\text{approx}} - V_{\text{removed}}$$

where V_{removed} is the total value of the removed items. It follows that:

$$V_{\text{OPT}} - V_{\text{removed}} \leq V_H.$$

According to Assumption 1, even if k items are removed, the total value loss is bounded. Consequently, the final additive error bound is

$$V_{\text{OPT}} - V_H \leq k \cdot v_{\max} \leq n \cdot v_{\max}$$

where $v_{\max}$ is the maximum value of a single item. The above derivation process proves that the gap between our solution and the true final solution is bounded, ensuring the robustness of the method. The computational complexity of Algorithm 4 is primarily dominated by the DP solver, which is

$$O\left(n \cdot W'\right) = O\left(n \cdot K \cdot W\right)$$

where n is the number of items and W represents the original capacity. The scaling factor K directly controls the tradeoff between accuracy and computation time: a larger K provides higher precision but increases the computation time.

Assumption 2: Discrete Weights. The amount of data is inherently discrete. In digital systems, data is usually managed in units of data packets, and memory is allocated in units of fixed-size blocks. Therefore, all weights w_j and capacity W can be expressed as integer multiples of a certain basic data unit $\Delta w > 0$.

3) Lossless Quantization: If we choose $K = 1/\Delta w$, the quantization is lossless. The original constraint $\sum w_j x_j \leq W$ is completely consistent with the integer constraint. In this case, DP can directly obtain the exact optimal solution

$$V_{\text{approx}} = V_{\text{OPT}}.$$

At this point, the quantization error is 0, and the time complexity of the DP algorithm is $O(n \cdot W/\Delta_w)$.

4) Lossy Quantization: In practical applications, a smaller K is usually used to improve efficiency, which will introduce some errors. According to the properties of the floor function, we have $\mathrm{K}w_j < \lfloor \mathrm{K}w_j \rfloor + 1$. Summing over the optimal solution S_{approx} of the quantization problem

$$W_{\text{real}}\left(S_{\text{approx}}\right) = \sum_{j \in S_{\text{approx}}} w_j < \sum_{j \in S_{\text{approx}}} \frac{\lfloor \mathrm{K}w_j \rfloor + 1}{K} = \frac{1}{K}\left(\sum_{j \in S_{\text{approx}}} \lfloor \mathrm{K}w_j \rfloor + |S_{\text{approx}}|\right). \tag{33}$$

Since $\sum \lfloor \mathrm{K}w_j \rfloor \leq KW$ and $|S_{\text{approx}}| \leq n$, we can obtain

$$W_{\text{real}}\left(S_{\text{approx}}\right) < \frac{1}{K}\left(KW + n\right) = W + \frac{n}{K}.$$

Under the premise of Assumption 2, any overweight $W_{\text{real}} - W$ must be a multiple of Δ_w. Therefore, the maximum overweight is

$$\delta_{\max} = \left\lfloor \frac{n-1}{K\Delta_w} \right\rfloor \cdot \Delta_w.$$

Next, we utilize the known properties of the 0–1 knapsack value function to obtain

$$V_{\mathrm{OPT}}(C_2) - V_{\mathrm{OPT}}(C_1) \le (C_2 - C_1) \cdot \rho_{\max} + v_{\max}.$$

Since $V_{\mathrm{OPT}}(W) \le V_{\mathrm{approx}} \le V_{\mathrm{OPT}}(W + \delta_{\max})$, the additive error bound can be expressed as follows:

$$V_{\mathrm{approx}} - V_{\mathrm{OPT}}(W) \le \left(\left\lfloor \frac{n-1}{K\Delta_w} \right\rfloor \cdot \Delta_w \right) \cdot \rho_{\max} + v_{\max}.$$

Under reasonable assumptions, we have conducted a rigorous theoretical analysis of the additive error. It is proven that the quantization method can ensure that the quality of the solution is close to the true optimal solution while significantly improving the computational efficiency.

VI. Experiment and Analysis

To validate the effectiveness and practicality of our proposed Quesada framework, we conduct a comprehensive set of experiments. Our evaluation is twofold: 1) we deploy Quesada on a physical end-edge–cloud prototype to demonstrate its viability and performance in a real-world setting and 2) we conducted large-scale simulations to evaluate the scalability and robustness of our framework in various 6G-IoT-like settings. Throughout the experiments, we focused on measuring the tradeoff between system reliability and data trustworthiness. We assessed reliability by looking at metrics such as running time and resource utilization. In parallel, we evaluated trustworthiness and the freshness of the cloud-side data.

A. Baseline Introduction

We compare our proposed approach, APX, against a suite of representative baselines, each embodying a different philosophical approach to the data acquisition problem.

1) QMIP and 2) QMIPR: These represent the theoretical oracle baselines. QMIP solves the original problem to find the true optimal solution using computationally expensive solvers (e.g., CPLEX), establishing the theoretical upper bound on performance. QMIPR is its relaxed version. They serve as a benchmark for optimality, against which we measure the efficacy of more practical approaches, but are themselves intractable for real-time 6G-IoT systems.
3) AM: This represents a centralized iterative optimization approach. As detailed in Algorithm 1, it requires a central controller with global knowledge to iteratively find a solution. While more efficient than QMIP, its centralized nature introduces a single point of failure and significant communication overhead, posing a reliability risk in distributed 6G-IoT.
4) RND: This is the naive, strategy-agnostic baseline. It makes random decisions for both edge collection and cloud synchronization. It serves as a performance floor, highlighting the substantial gains achieved through intelligent control.
5) BZ8G (Busy Edge): This embodies an aggressive, trustworthiness-first heuristic. It relentlessly collects data from all devices ($\rho_{t,i,j} = 1$) to maximize data freshness. This approach completely neglects resource constraints, inevitably leading to network congestion and device energy depletion, thereby severely compromising long-term system reliability.
6) IPTC (Importance): This is a static, priority-based heuristic. It allocates resources based on the predefined importance of data sources. While more intelligent than RND, it is static and cannot adapt to the dynamic changes in network conditions or data states, failing to strike an optimal balance between reliability and trustworthiness.
7) BASE: It is a priority-free sequential filling algorithm based on the "first-come and first-served" principle. During the cloud synchronization phase, this algorithm does not calculate the "trustworthiness value" or "importance" of any data. Instead, it selects data for synchronization in a fixed and meaningless order until the total cloud synchronization capacity $\mathtt{D}^\star$ is exhausted. The flaw of this method lies in its undifferentiated decision-making.
8) APX (Our Approach): This is our proposed decoupled and adaptive framework. By decomposing the problem and employing efficient, distributed algorithms (see Algorithms 2 and 3), it is designed to pragmatically balance the reliability-trustworthiness tradeoff in a scalable and efficient manner, making it suitable for practical 6G-IoT deployments.

B. Comparisons on Raspberry Pi-Based Prototype

We first validate Quesada's performance on the physical testbed shown in Fig. 2. This experiment is crucial for demonstrating the framework's practical viability beyond theoretical simulations. Fig. 3 presents the results.

The analysis clearly demonstrates the superiority of our APX framework. In terms of trustworthiness, APX achieves the highest cloud-side data freshness ($\mathcal{F}$), ensuring that high-level AI applications operate on the most accurate global information. Simultaneously, its edge-side AoI ($\mathcal{A}^*$) is comparable to the computationally prohibitive oracle methods (QMIP, AM), indicating the excellent edge-side data trustworthiness.

From a reliability perspective, the advantages are even more pronounced. The running time of APX is orders of magnitude lower than the oracle and centralized methods, proving its feasibility for real-time decision-making, a cornerstone of operational reliability in dynamic 6G networks. Furthermore, its 100% constraint compliance rate underscores its robustness in resource management. Unlike BZ8G or RND which frequently violate system limits, APX guarantees stable operation within the predefined cache and bandwidth budgets, preventing system instability. In summary, APX provides the best overall balance, delivering near-optimal trustworthiness with superior reliability and efficiency.

C. Problem Scale Versus Performance

We now evaluate the scalability of Quesada, a critical attribute for any framework targeting the massive connectivity of 6G-IoT. We use simulations to assess performance as the number of edge servers and devices increases.

1) Impact of Edge Server Number: Fig. 4 shows the performance as the number of edge servers grows from

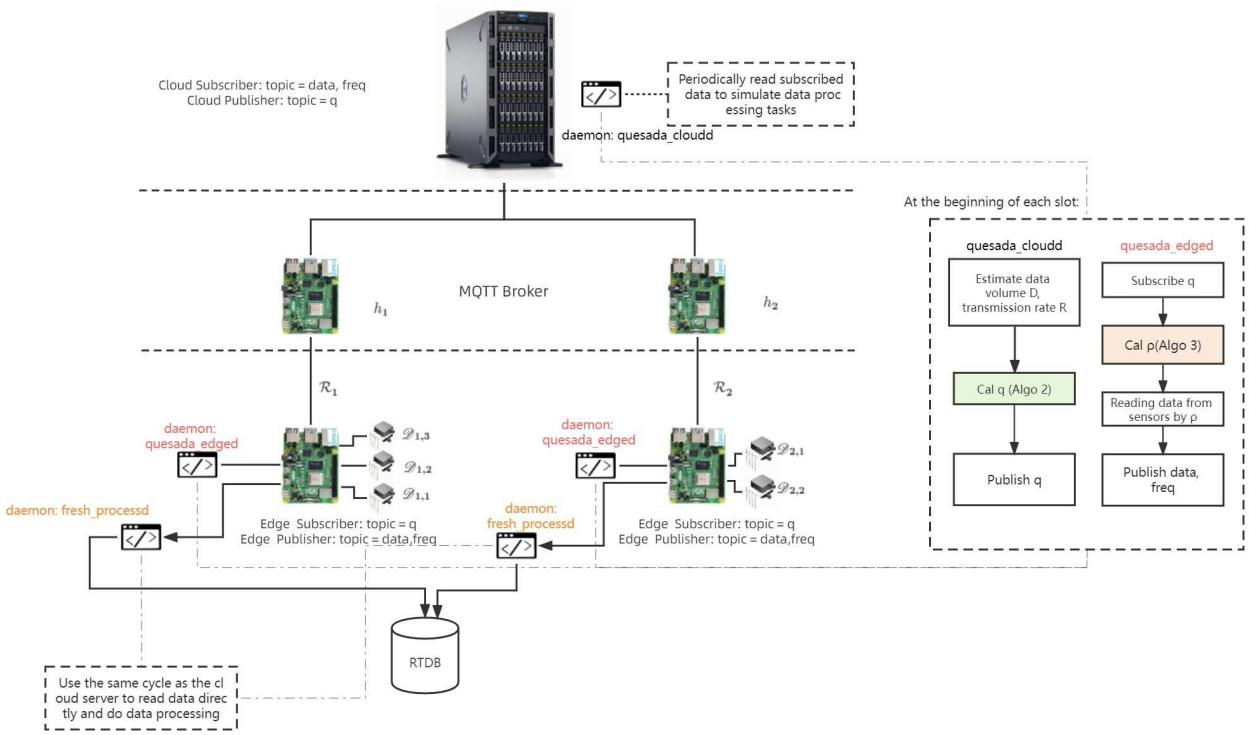

Fig. 2. Quesada framework implemented on a physical prototype with two Raspberry Pi (edge servers) and four sensors (end devices).

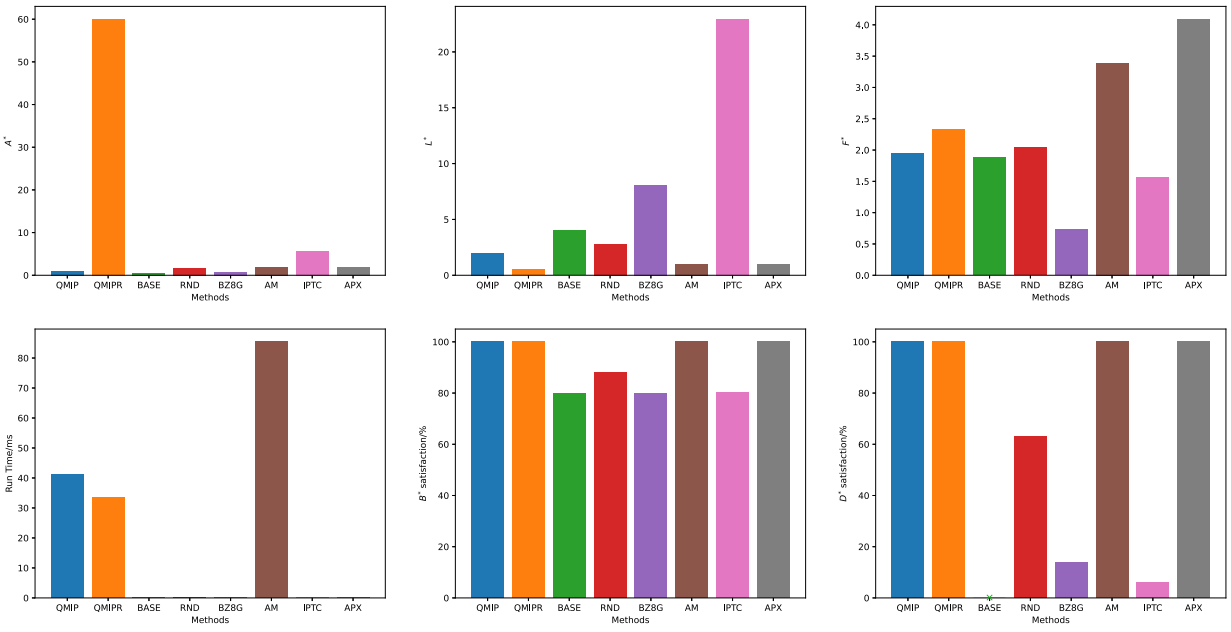

Fig. 3. Performance evaluation on the physical prototype, comparing key metrics for trustworthiness and reliability.

5 to 50. APX demonstrates superior horizontal scalability. While the performance of all methods degrades with scale, APX's metrics remain stable and significantly better than other practical heuristics. This proves the effectiveness of our distributed architecture in avoiding the communication bottlenecks and computational explosion that would plague centralized systems, highlighting its reliability in large-scale.

2) Impact of Device Number: Next, we increase the device density per edge server, simulating a more demanding data environment. As shown in Fig. 5, when the data load from the devices increases, our APX method does a better job of managing a difficult balance. On one hand, it works hard to keep the data fresh; this is the essence of what we call data trustworthiness. On the other hand, it avoids overwhelming the system, which is crucial for its system reliability. You

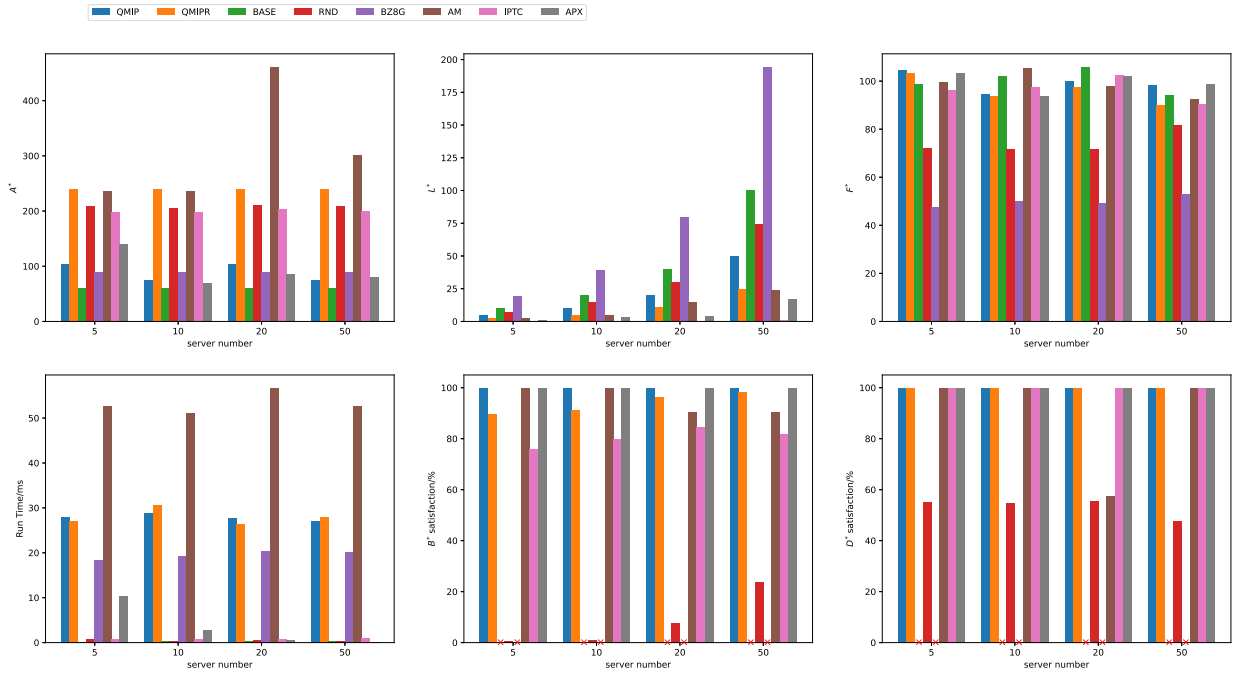

Fig. 4. Performance comparison as the number of edge servers increases, testing the framework's horizontal scalability.

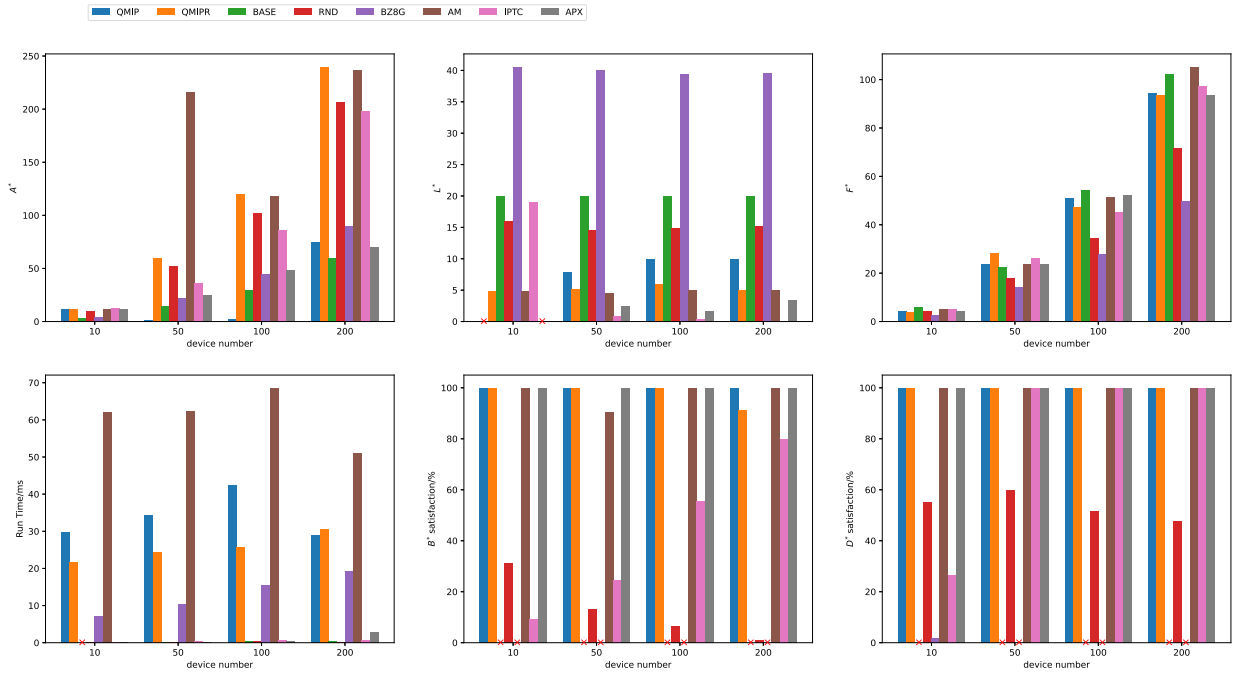

Fig. 5. Performance comparison as the number of devices per edge server increases, testing the framework's robustness against high data loads.

can see this in the AoI, freshness, and latency metrics, where APX consistently stays ahead of the others. This showcases its robustness against high data loads, a crucial feature for dense 6G-IoT scenarios like smart cities or industrial automation.

D. System Settings Versus Performance

This section investigates the adaptability of Quesada to varying system parameters, which represent different deployment scenarios and network conditions in 6G-IoT environments.

1) Impact of Edge Server Storage: Edge cache size $B^\star$ represents the resource reliability of an edge node. Fig. 6 shows that Quesada effectively leverages increased cache reliability to improve overall data trustworthiness. With more available storage, it can make more aggressive yet safe collection decisions, leading to a significant reduction in AoI ($\mathcal{A}^*$).

2) Impact of the Cloud: Cloud synchronization capacity ($D^\star$) reflects the reliability of the edge–cloud backhaul link. As shown in Fig. 7, our framework intelligently utilizes higher

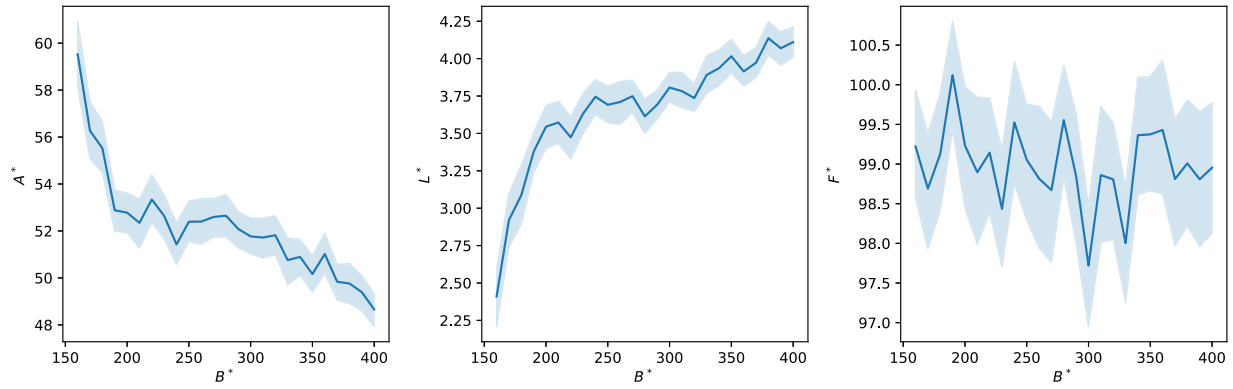

Fig. 6. Impact of edge cache capacity ($B^{\star}$), a measure of edge node resource reliability.

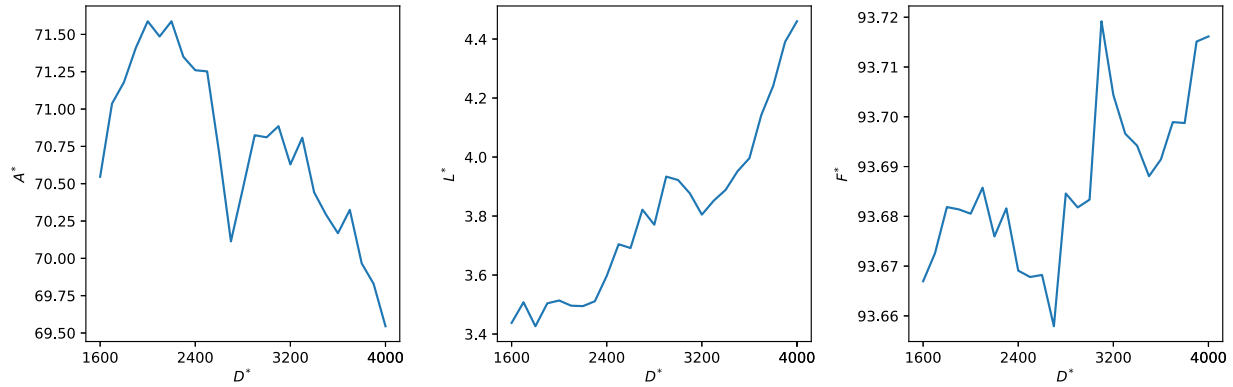

Fig. 7. Impact of cloud synchronization capacity ($D^{\star}$), a measure of edge–cloud backhaul reliability.

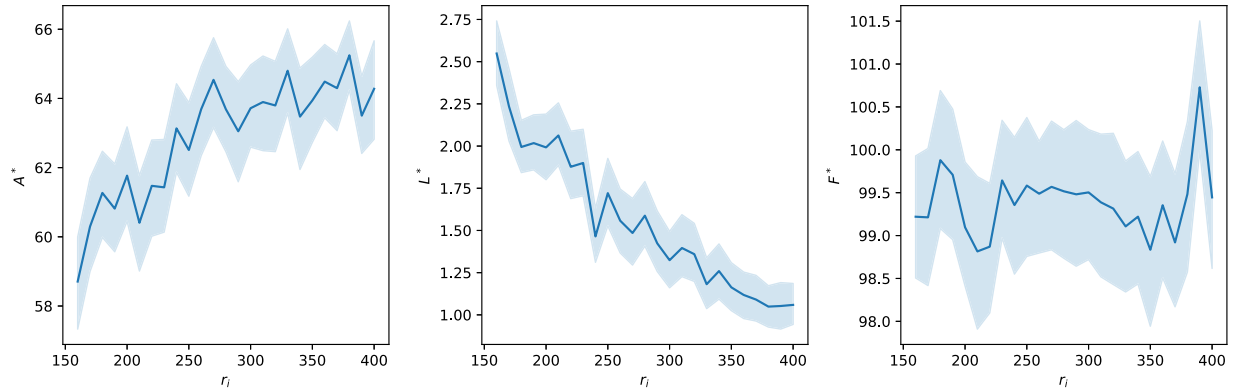

Fig. 8. Impact of transmission rate (r_i), a proxy for 6G network communication quality.

backhaul reliability to enhance global data trustworthiness ($\mathcal{F}$). A more capable cloud link allows for more frequent synchronization, ensuring the cloud's AI models have the freshest possible view of the entire system.

3) Impact of Communication Quality: The transmission rate (r_i) directly maps to the communication quality of the 6G network. Fig. 8 demonstrates that Quesada seamlessly adapts to improved network conditions. As communication becomes more reliable (higher r_i) and transmission latency ($\mathcal{L}$) naturally decreases. Our framework intelligently converts this network dividend into a better balance of system-wide metrics, showcasing its synergy with advanced network infrastructure.

4) Impact of Decision Duration: The time slot duration (δ) models the application's demand for decision frequency. A smaller δ represents a more dynamic, high-stakes environment. Fig. 9 shows that as the decision window shrinks, our framework makes a strategic tradeoff, slightly sacrificing optimal freshness to ensure decisions can be made within the time limit, thus prioritizing operational reliability.

5) Impact of Data Collecting Rate: The data generation rate (η) reflects the intensity of the application (e.g., low

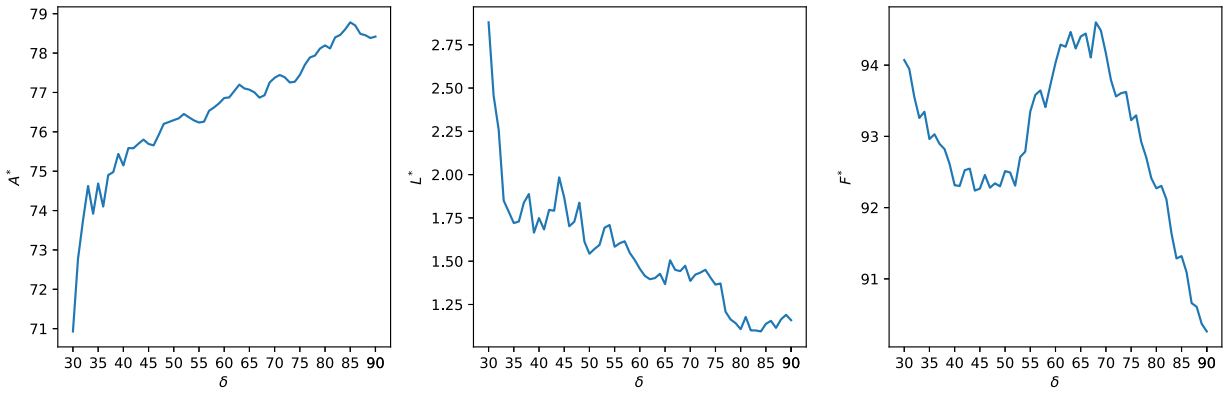

Fig. 9. Impact of decision slot duration (δ), modeling different application latency requirements.

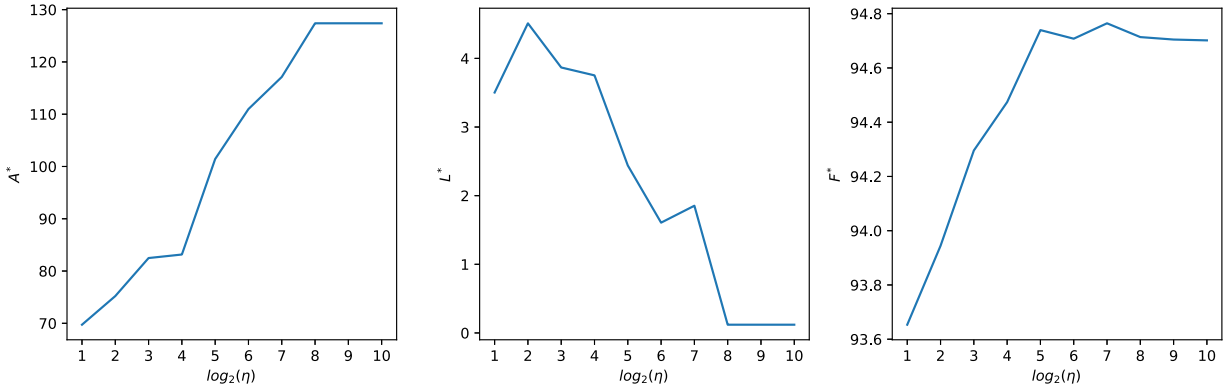

Fig. 10. Impact of data generation rate (η), modeling different data-intensive applications.

for temperature sensing and high for video streaming). As shown in Fig. 10, when faced with high-velocity data, Quesada intelligently reduces collection frequency. This demonstrates its crucial self-preservation behavior: it prioritizes fundamental system reliability (preventing data overload and system collapse) over chasing maximum data freshness, a vital feature for ensuring the stability of mission-critical IoT applications.

E. Scaling Factor Settings Versus Performance

To evaluate the performance of different scaling factors K in the quantization problem, we compared the efficiency of various algorithms when solving instances of the knapsack problem with different scales. Through this comparison, we can weigh and choose the most suitable algorithm.

1) Average Computation Time: Mixed-integer LP (MILP), as an exact solver, exhibits the longest computation time when handling large-scale problems. In contrast, the QSR series in **APX** generally demonstrates a significant efficiency advantage, with computation times far lower than those of MILP. This indicates that, as an approximate method, QSR can provide acceptable solutions while maintaining relatively high efficiency. According to the discussion in Section V regarding the scaling factor K, the computation time shows an upward trend as K increases. The greedy algorithms, due to their fast but not necessarily optimal nature, have become the ones with the shortest computation time among all algorithms.

2) Selection of Scaling Factor K: The line graph in Fig. 11 intuitively illustrates the impact of different K values on algorithm performance within the QSR framework. The experimental results show that as K increases, the average relative error of the QSR algorithm significantly decreases, which aligns with the theoretical analysis results discussed in Section V. When K = 100, the rate of error reduction begins to slow down. Specifically, larger K values imply more precise quantization of weights and capacities, making the results of DP closer to the optimal solution of the quantized problem. Therefore, by balancing runtime and solution accuracy, one can find the most suitable solution.

3) Summary of Algorithm Performance: The scatter plot in Fig. 11 integrates the two key dimensions of error and computation time into a single chart. From the figure, it can be seen that MILP is located in the bottom-right corner, representing a strategy that seeks extreme precision at the cost of efficiency, whereas the QSR series of algorithms forms a curve from the top left to the bottom right, indicating that users can flexibly choose between precision and efficiency based on their needs. It is particularly noteworthy that when striving for a good balance between precision and efficiency, the QSR algorithm demonstrates strong competitiveness. By adjusting the factor $K = 100$, one can achieve reasonable accuracy with moderate computation time.

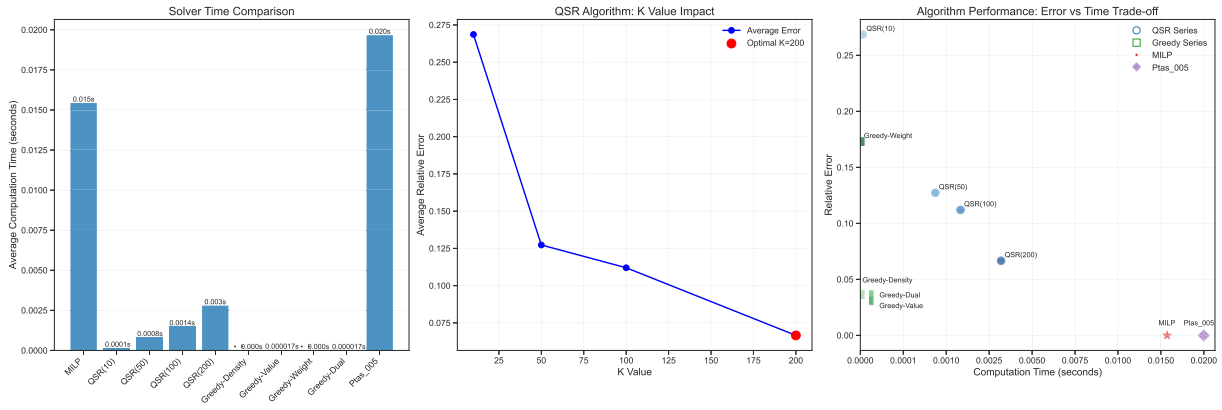

Fig. 11. Performance of different approximate algorithms.

F. Approximation Approaches Versus Performance

Traditionally, the PTAS [43] algorithm is commonly employed to solve the general knapsack problem, enabling a flexible tradeoff between solution quality and running time through an error parameter ε. Unlike the proposed QSR algorithm within the APX, PTAS achieves this by quantizing item values—scaling and rounding them to reduce the range of possible profits—thereby transforming the original problem into a simplified variant amenable to efficient DP. This transformation guarantees a polynomial-time approximation whose relative error with respect to the optimal solution is bounded by ε. For instance, when $\varepsilon = 0.05$, PTAS ensures that the approximate solution's objective value is within 5% of the true optimum. While this level of accuracy often surpasses the feasible solutions obtained by traditional MILP solvers under time constraints, PTAS typically exhibits significantly longer runtime than standard MILP solvers on problems of comparable scale, as illustrated in the left bar chart and right scatter plot of Fig. 11. This is reasonable, as classical MILP solvers have been extensively optimized over decades of research and engineering effort. Unless the problem scale reaches millions of items, a state-of-the-art MILP solver will usually find the exact optimal solution faster and with far less implementation complexity than a PTAS implementation. In other words, while PTAS offers strong theoretical guarantees on solution quality, it incurs substantial practical computational overhead, making it most suitable for scenarios where high accuracy is paramount and longer runtimes are acceptable. In contrast, the QSR algorithms more effectively exploit the discrete structure of resources, achieving a superior balance between solution accuracy and computational efficiency.

VII. Conclusion

In summary, this article conducts a thorough investigation into the data acquisition problem, a critical component for ensuring the reliability and trustworthiness of AI services in future 6G-IoT collaborative scenarios. By formally modeling the tradeoff between system reliability, which is quantified by transmission costs and resource constraints) and data trustworthiness, which is measured by information freshness, we formulate the challenge as a unified optimization problem.

An analysis of this formulated problem reveals its high computational complexity, making it difficult to obtain optimal solutions in real time. Therefore, we propose an efficient and practical approximated approach, named APX. This approach decouples the problem into two manageable subproblems, which are then solved separately using greedy and DP techniques to achieve a near-optimal solution with significantly reduced computational overhead.

Experimental results demonstrate that the APX consistently outperforms other representative approaches, achieving a superior balance between maintaining high data trustworthiness and ensuring system reliability. Furthermore, our extensive parameter analysis explores how various system configurations impact overall performance, providing valuable insights for practical system deployment and optimization. This lays a solid foundation for future research on more advanced strategies for building dependable and trustworthy data pipelines in the 6G-IoT landscape.

Now, we can address how the framework proposed in this article solves the two issues raised in Section II. Regarding question *Q1*, "Is it necessary to query every end-device?" the Quesada provides a solution through its AoI-based edge-side data collection strategy. It balances information freshness with system reliability, avoiding the energy consumption problem caused by indiscriminate queries to all devices. For question *Q2*, "How often should data be synchronized with the cloud?," the Quesada treats data synchronization as a continuous knapsack problem. It adopts a greedy algorithm to prioritize synchronizing data with higher trustworthiness density, maximizing the freshness of cloud-side data without exceeding the cloud's synchronization capacity.

In future work, we plan to explore learning-based approaches—particularly RL—to dynamically adapt resource allocation strategies in response to changing system conditions. Recent advances in data-driven optimization [44], [45], and adaptive learning frameworks [46] suggest that RL can effectively learn near-optimal control policies for complex, dynamic environments without explicit modeling of the underlying constraints. Specifically, we aim to investigate how model-free or model-based RL algorithms [47] can be integrated into our framework to autonomously tune parameters in real time, thereby improving both solution

quality and computational efficiency in online or stochastic settings.

ACKNOWLEDGMENT

Zhengzhe Xiang was instrumental in proposing the framework concept and the approaches. Zhengzhe Xiang, Rong Tan, and Schahram Dustdar played significant roles in problem modeling. Zhengzhe Xiang and Yufei Zhang wrote this article. Fuli Ying and Dezhi Wang conducted the experiments. The language of this article was polished with the assistance of Gemini[1] and Qwen.[2]

REFERENCES

[1] S. Dang, O. Amin, B. Shihada, and M.-S. Alouini, "What should 6G be?," *Nature Electron.*, vol. 3, no. 1, pp. 20–29, Jan. 2020.

[2] C.-X. Wang et al., "On the road to 6G: Visions, requirements, key technologies, and testbeds," *IEEE Commun. Surveys Tuts.*, vol. 25, no. 2, pp. 905–974, 2nd Quart. 2023.

[3] J. Laux, S. Wachter, and B. Mittelstadt, "Trustworthy artificial intelligence and the European union AI act: On the conflation of trustworthiness and acceptability of risk," *Regulation Governance*, vol. 18, no. 1, pp. 3–32, Jan. 2024.

[4] C. G. García, E. R. Núñez-Valdéz, V. García-Díaz, B. C. P. García-Bustelo, and J. M. C. Lovelle, "A review of artificial intelligence in the Internet of Things," *Int. J. Interact. Multimedia Artif. Intell.*, vol. 5, no. 4, p. 9, 2018.

[5] Y. Wang, H. Gao, Z. Xiang, Z. Zhu, and A. Al-Dulaimi, "RSMR: A reliable and sustainable multi-path routing scheme for vehicle electronics in edge computing networks," *IEEE Trans. Consum. Electron.*, vol. 71, no. 1, pp. 2090–2106, Feb. 2025.

[6] T. Liang, M. Chen, Y. Yin, L. Zhou, and H. Ying, "Recurrent neural network based collaborative filtering for QoS prediction in IoV," *IEEE Trans. Intell. Transp. Syst.*, vol. 23, no. 3, pp. 2400–2410, Mar. 2022.

[7] Y. Chen, F. Zhao, X. Chen, and Y. Wu, "Efficient multi-vehicle task offloading for mobile edge computing in 6G networks," *IEEE Trans. Veh. Technol.*, vol. 71, no. 5, pp. 4584–4595, May 2022.

[8] J. Zhang and D. Tao, "Empowering things with intelligence: A survey of the progress, challenges, and opportunities in artificial intelligence of things," *IEEE Internet Things J.*, vol. 8, no. 10, pp. 7789–7817, May 2021.

[9] B. Dong, Q. Shi, Y. Yang, F. Wen, Z. Zhang, and C. Lee, "Technology evolution from self-powered sensors to AIoT enabled smart homes," *Nano Energy*, vol. 79, Jan. 2021, Art. no. 105414.

[10] H. Liazid, M. Lehsaini, and A. Liazid, "Data transmission reduction using prediction and aggregation techniques in IoT-based wireless sensor networks," *J. Netw. Comput. Appl.*, vol. 211, Feb. 2023, Art. no. 103556.

[11] A. Singh and A. Nagaraju, "Low latency and energy efficient routing-aware network coding-based data transmission in multi-hop and multi-sink WSN," *Ad Hoc Netw.*, vol. 107, Oct. 2020, Art. no. 102182.

[12] A. S. Nandan, S. Singh, A. Malik, and R. Kumar, "A green data collection & transmission method for IoT-based WSN in disaster management," *IEEE Sensors J.*, vol. 21, no. 22, pp. 25912–25921, Nov. 2021.

[13] P. Maheshwari, A. K. Sharma, and K. Verma, "Energy efficient cluster based routing protocol for WSN using butterfly optimization algorithm and ant colony optimization," *Ad Hoc Netw.*, vol. 110, Jan. 2021, Art. no. 102317.

[14] M. Yi, X. Wang, J. Liu, Y. Zhang, and B. Bai, "Deep reinforcement learning for fresh data collection in UAV-assisted IoT networks," in *Proc. IEEE Conf. Comput. Commun. Workshops (INFOCOM WKSHPS)*, Jul. 2020, pp. 716–721.

[15] X. Gao, X. Zhu, and L. Zhai, "AoI-sensitive data collection in multi-UAV-assisted wireless sensor networks," *IEEE Trans. Wireless Commun.*, vol. 22, no. 8, pp. 5185–5197, Aug. 2023.

[16] X. Li, J. Tan, A. Liu, P. Vijayakumar, N. Kumar, and M. Alazab, "A novel UAV-enabled data collection scheme for intelligent transportation system through UAV speed control," *IEEE Trans. Intell. Transp. Syst.*, vol. 22, no. 4, pp. 2100–2110, Apr. 2021.

[1]https://gemini.google.com

[2]https://chat.qwen.ai

[17] S. Li, F. Wu, S. Luo, Z. Fan, J. Chen, and S. Fu, "Dynamic online trajectory planning for a UAV-enabled data collection system," *IEEE Trans. Veh. Technol.*, vol. 71, no. 12, pp. 13332–13343, Dec. 2022.

[18] Y. Li et al., "Data collection maximization in IoT-sensor networks via an energy-constrained UAV," *IEEE Trans. Mobile Comput.*, vol. 22, no. 1, pp. 159–174, Jan. 2023.

[19] C. Kai, H. Zhou, Y. Yi, and W. Huang, "Collaborative cloud-edge-end task offloading in mobile-edge computing networks with limited communication capability," *IEEE Trans. Cognit. Commun. Netw.*, vol. 7, no. 2, pp. 624–634, Jun. 2021.

[20] S. Tian, C. Chang, S. Long, S. Oh, Z. Li, and J. Long, "User preference-based hierarchical offloading for collaborative cloud-edge computing," *IEEE Trans. Services Comput.*, vol. 16, no. 1, pp. 684–697, Jan. 2023.

[21] J. Huang, J. Wan, B. Lv, Q. Ye, and Y. Chen, "Joint computation offloading and resource allocation for edge-cloud collaboration in Internet of Vehicles via deep reinforcement learning," *IEEE Syst. J.*, vol. 17, no. 2, pp. 2500–2511, Jun. 2023.

[22] X. Wang and G. Gao, "SmartEye: An open source framework for real-time video analytics with edge-cloud collaboration," in *Proc. 29th ACM Int. Conf. Multimedia*, Oct. 2021, pp. 3767–3770.

[23] S. Long, Y. Zhang, Q. Deng, T. Pei, J. Ouyang, and Z. Xia, "An efficient task offloading approach based on multi-objective evolutionary algorithm in cloud-edge collaborative environment," *IEEE Trans. Netw. Sci. Eng.*, vol. 10, no. 2, pp. 645–657, Mar. 2023.

[24] L. Li, D. Shi, R. Hou, H. Li, M. Pan, and Z. Han, "To talk or to work: Flexible communication compression for energy efficient federated learning over heterogeneous mobile edge devices," in *Proc. IEEE Conf. Comput. Commun.*, May 2021, pp. 1–10.

[25] M. Li, N. Cheng, J. Gao, Y. Wang, L. Zhao, and X. Shen, "Energy-efficient UAV-assisted mobile edge computing: Resource allocation and trajectory optimization," *IEEE Trans. Veh. Technol.*, vol. 69, no. 3, pp. 3424–3438, Mar. 2020.

[26] L. Ale, N. Zhang, X. Fang, X. Chen, S. Wu, and L. Li, "Delay-aware and energy-efficient computation offloading in mobile-edge computing using deep reinforcement learning," *IEEE Trans. Cognit. Commun. Netw.*, vol. 7, no. 3, pp. 881–892, Sep. 2021.

[27] F. Wang, J. Xu, and S. Cui, "Optimal energy allocation and task offloading policy for wireless powered mobile edge computing systems," *IEEE Trans. Wireless Commun.*, vol. 19, no. 4, pp. 2443–2459, Apr. 2020.

[28] S. Xia, Z. Yao, Y. Li, and S. Mao, "Online distributed offloading and computing resource management with energy harvesting for heterogeneous MEC-enabled IoT," *IEEE Trans. Wireless Commun.*, vol. 20, no. 10, pp. 6743–6757, Oct. 2021.

[29] W. Zhou, L. Xing, J. Xia, L. Fan, and A. Nallanathan, "Dynamic computation offloading for MIMO mobile edge computing systems with energy harvesting," *IEEE Trans. Veh. Technol.*, vol. 70, no. 5, pp. 5172–5177, May 2021.

[30] F. Zhao, Y. Chen, Y. Zhang, Z. Liu, and X. Chen, "Dynamic offloading and resource scheduling for mobile-edge computing with energy harvesting devices," *IEEE Trans. Netw. Service Manage.*, vol. 18, no. 2, pp. 2154–2165, Jun. 2021.

[31] S. Wang, Y. Zhao, J. Xu, J. Yuan, and C.-H. Hsu, "Edge server placement in mobile edge computing," *J. Parallel Distrib. Comput.*, vol. 127, pp. 160–168, May 2019.

[32] Q. He et al., "EDIndex: Enabling fast data queries in edge storage systems," in *Proc. 46th Int. ACM SIGIR Conf. Res. Develop. Inf. Retr.*, Jul. 2023, pp. 675–685.

[33] B. Tang, F. Guo, B. Cao, M. Tang, and K. Li, "Cost-aware deployment of microservices for IoT applications in mobile edge computing environment," *IEEE Trans. Netw. Service Manage.*, vol. 20, no. 3, pp. 3119–3134, Sep. 2023.

[34] Z. Xiang, Y. Zheng, Z. Zheng, S. Deng, M. Guo, and S. Dustdar, "Cost-effective traffic scheduling and resource allocation for edge service provisioning," *IEEE/ACM Trans. Netw.*, vol. 31, no. 6, pp. 2934–2949, Dec. 2023.

[35] Y. Jia, C. Zhang, Y. Huang, and W. Zhang, "Lyapunov optimization based mobile edge computing for Internet of Vehicles systems," *IEEE Trans. Commun.*, vol. 70, no. 11, pp. 7418–7433, Nov. 2022.

[36] A. Kosta, N. Pappas, and V. Angelakis, "Age of information: A new concept, metric, and tool," *Found. Trends Netw.*, vol. 12, no. 3, pp. 162–259, 2017.

[37] A. Kolobov, Y. Peres, E. Lubetzky, and E. Horvitz, "Optimal freshness crawl under politeness constraints," in *Proc. 42nd Int. ACM SIGIR Conf. Res. Develop. Inf. Retr.*, Jul. 2019, pp. 495–504.

[38] G. Ahani and D. Yuan, "Optimal content caching and recommendation with age of information," *IEEE Trans. Mobile Comput.*, vol. 23, no. 1, pp. 689–704, Jan. 2022.
[39] Z. Fang, J. Wang, Y. Ren, Z. Han, H. V. Poor, and L. Hanzo, "Age of information in energy harvesting aided massive multiple access networks," *IEEE J. Sel. Areas Commun.*, vol. 40, no. 5, pp. 1441–1456, May 2022.
[40] S. Yun, D. Kim, C. Park, and J. Lee, "Learning-based sensing and computing decision for data freshness in edge computing-enabled networks," *IEEE Trans. Wireless Commun.*, vol. 23, no. 9, pp. 11386–11400, Sep. 2024.
[41] I. J. Lustig, R. E. Marsten, and D. F. Shanno, "Interior point methods for linear programming: Computational state of the art," *ORSA J. Comput.*, vol. 6, no. 1, pp. 1–14, 1994.
[42] T. H. Cormen, C. E. Leiserson, R. L. Rivest, and C. Stein, *Introduction to Algorithms*, 4th ed., Cambridge, MA, USA: MIT Press, 2022.
[43] C. Chekuri and S. Khanna, "A polynomial time approximation scheme for the multiple knapsack problem," *SIAM J. Comput.*, vol. 35, no. 3, pp. 713–728, Jan. 2005.
[44] Y. Huang, H. Xu, Q. Ran, W. Wei, and H. Gao, "GRWS: A deep reinforcement learning method with graph attention networks for flexible workflow scheduling in industrial manufacturing scenarios," *IEEE Internet Things J.*, early access, Apr. 29, 2025, doi: 10.1109/JIOT.2025.3565325.
[45] P. Li, Z. Xiao, H. Gao, X. Wang, and Y. Wang, "Reinforcement learning based edge-end collaboration for multi-task scheduling in 6G enabled intelligent autonomous transport systems," *IEEE Trans. Intell. Transp. Syst.*, early access, Jan. 16, 2025, doi: 10.1109/TITS.2024.3525356.
[46] C. Zhang, Y. Deng, H. Zhao, T. Chen, and S. Deng, *Tail-Learning: Adaptive Learning Method for Mitigating Tail Latency in Autonomous Edge Systems*. New York, NY, USA: Association for Computing Machinery, May 2025, doi: 10.1145/3737289.
[47] H. Zeng, Z. Zhu, Y. Wang, Z. Xiang, and H. Gao, "Periodic collaboration and real-time dispatch using an actor–critic framework for UAV movement in mobile edge computing," *IEEE Internet Things J.*, vol. 11, no. 12, pp. 21215–21226, Jun. 2024.

Zhengzhe Xiang received the B.S. and Ph.D. degrees from Zhejiang University, Hangzhou, China, in 2013 and 2020, respectively.

He was a Visiting Scholar with Shanghai Jiao Tong University, Shanghai, China, in 2022. He is currently an Associate Professor with Hangzhou City University, Hangzhou. His research interests lie in the fields of service computing and edge computing.

Dr. Xiang serves as a reviewer for several international journals, such as IEEE TRANSACTIONS ON MOBILE COMPUTING (TMC), IEEE TRANSACTIONS ON SERVICES COMPUTING (TSC), and IEEE/ACM TRANSACTIONS ON NETWORKING (TNET). He also serves as a PC member for many international conferences.

Fuli Ying is currently pursuing the master's degree with the School of Computer and Computing Sciences, Hangzhou City University, Hangzhou, China.

Her research interests encompass mobile edge computing, deep learning architectures, and image processing, with a focus on developing efficient algorithms for distributed computing environments and intelligent visual analysis systems.

Dezhi Wang received the M.S. degree from the College of Computer Science and Technology, Zhejiang University, Hangzhou, China, in 2024.

He is currently with the Alibaba Group, Hangzhou, China. His research interests include the Internet of Things technology, edge computing, service computing, and reinforcement learning.

Rong Tan received the Ph.D. degree from East China Normal University, Shanghai, China, in 2013,

He worked as a Post-Doctoral Research Associate at Beijing Tehua Postdoctoral Programme. He is currently an Associate Professor with the Internet of Things Engineering Department, Shanghai Business School, Shanghai. His research interests include cloud/edge computing and blockchain.

Yufei Zhang was born in Zhuji, Zhejiang, China, in 1990. She received the Ph.D. degree from Zhejiang University, Hangzhou, China, in 2022.

She is currently a Lecturer with Hangzhou City University, Hangzhou. Her current research interests include service computing, generative artificial intelligence, and bionics.

Schahram Dustdar (Fellow, IEEE) is currently a Full Professor of computer science and the Head of the Distributed Systems Group, TU Wien, Vienna, Austria. His research interests include distributed systems, edge intelligence, complex and autonomic software systems.

Dr. Dustdar is a fellow of AAIA, where he is currently the President. He is the Editor-In-Chief of *Computing*; an Associate Editor of *ACM Transactions on the Web*, *ACM Transactions on Internet Technology*, IEEE TRANSACTIONS ON CLOUD COMPUTING, and IEEE TRANSACTIONS ON SERVICES COMPUTING. He is also on the editorial boards of IEEE INTERNET COMPUTING and *Computer*. He has received the ACM Distinguished Scientist Award, and Distinguished Speaker Award, and the IBM Faculty Award. He is an Elected Member of Academia Europaea, where he was Informatics Section Chairman from 2015 to 2022.